

# Presence and stability of rotors in atrial fibrillation: evidence and therapeutic implications

María S. Guillem<sup>1</sup>, Andreu M. Climent<sup>2,3</sup>, Miguel Rodrigo<sup>1</sup>,  
Francisco Fernández-Avilés<sup>2,3,4</sup>, Felipe Atienza<sup>2,3,4†</sup>, and Omer Berenfeld<sup>5\*†</sup>

<sup>1</sup>ITACA, Universitat Politècnica de València, Valencia, Spain; <sup>2</sup>Hospital General Universitario Gregorio Marañón, Madrid, Spain; <sup>3</sup>Instituto de Investigación Sanitaria Gregorio Marañón, Madrid, Spain; <sup>4</sup>Facultad de Medicina, Universidad Complutense de Madrid, Spain; and <sup>5</sup>Center for Arrhythmia Research, University of Michigan, 2800 Plymouth Road, Ann Arbor, MI 48109, USA

Received 11 October 2015; revised 30 December 2015; accepted 15 January 2016; online publish-ahead-of-print 19 January 2016

## Abstract

Rotor-guided ablation has opened new perspectives into the therapy of atrial fibrillation (AF). Analysis of the spatio-temporal cardiac excitation patterns in the frequency and phase domains has demonstrated the importance of rotors in research models of AF, however, the dynamics and role of rotors in human AF are still controversial. In this review, the current knowledge gained through research models and patient data that support the notion that rotors are key players in AF maintenance is summarized. We report and discuss discrepancies regarding rotor prevalence and stability in various studies, which can be attributed in part to methodological differences among mapping systems. Future research for validation and improvement of current clinical electrophysiology mapping technologies will be crucial for developing mechanistic-based selection and application of the best therapeutic strategy for individual AF patient, being it, pharmaceutical, ablative, or other approach.

## Keywords

Atrial fibrillation • Body surface mapping • Rotors • Dominant frequency • Fourier transform • Phase mapping

This article is part of the Spotlight Issue on atrial fibrillation.

## 1. Introduction

Atrial fibrillation (AF) is the most common arrhythmia seen in clinical practice and is associated with increased risk of stroke, heart failure, and death.<sup>1</sup> Despite intense efforts, the success of current therapies for restoring sinus rhythm in AF patients by administration of anti-arrhythmic drugs, electrical cardioversion, or catheter ablation is suboptimal.

Catheter ablation has emerged as a more effective approach in maintaining sinus rhythm than anti-arrhythmic drugs,<sup>2–4</sup> with reported success rates of ~70%.<sup>5</sup> However, catheter ablation is not free from procedural complications, and up to 4.5% of the patients develop major complications including tamponade (1.31%), femoral pseudoaneurysm (0.93%), transient ischaemia (0.71%), and death (0.15%).<sup>5</sup>

Following the identification of the major role of pulmonary veins (PVs) in the initiation of AF,<sup>6</sup> PV isolation (PVI) has been established as the recommended catheter ablation approach<sup>7</sup> with overall success rates of up to 87% in paroxysmal AF patients.<sup>8–10</sup> However, up to 43% of paroxysmal AF patients may develop AF recurrence after a repeat procedure if anti-arrhythmic drugs are discharged.<sup>10,11</sup> Moreover, success rates of catheter ablation in non-paroxysmal AF patients are

disappointing, with AF-free rates for a single procedure as low as 28%, or 51% for multiple repeat procedures.<sup>12</sup>

As opposed to the anatomical-only PVI strategy, ablation approaches that target AF sources have also been proposed. Isolation of atrial sources identified as those that could initiate AF after stimulation<sup>13</sup> or as those with highest activation rates<sup>14</sup> has been reported to be as efficient as isolation of all PVs. Recent reports on the efficiency of rotor-based ablation strategies, which can outperform PVI,<sup>15–17</sup> highlight the discussion on the dynamics of rotors and their role in AF maintenance to further the development of mechanistic-based therapies on an individual patient basis.

## 2. Mechanisms of AF and rotor definition

There is still an open debate regarding the mechanisms that initiate and maintain AF.<sup>18,19</sup> Although some investigators advocate for the presence of multiple wavelets with a random propagation as the main mechanism sustaining AF,<sup>20,21</sup> other investigators argue that there are spatially localized drivers in the form of rotors that maintain the

\* Corresponding author. Tel: +1 734 998 7560; Fax: +1 734 998 7711, Email: oberen@umich.edu

† F.A. and O.B. share senior authorship.

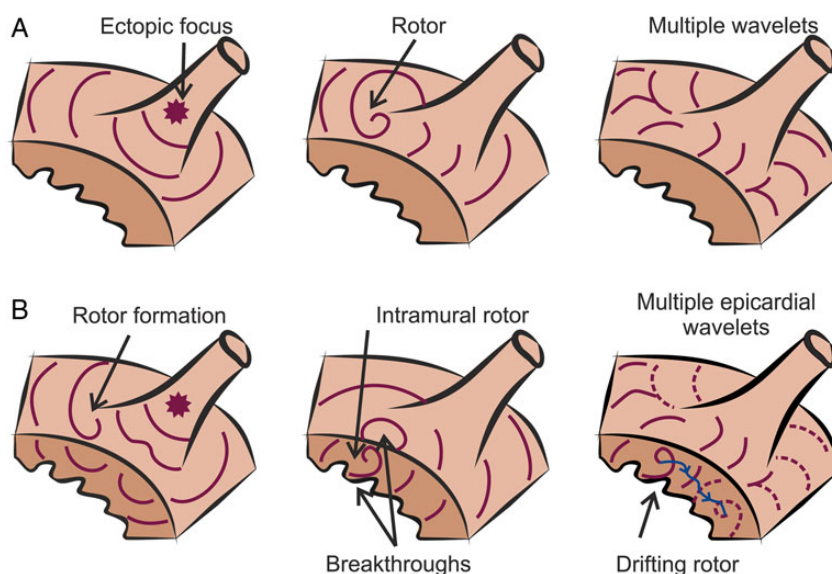


**Figure 1** Current hypothesis for AF maintenance. (A) Diagram of AF maintenance near a PV that has been hypothesized to be driven by ectopic focus (left), rotors (middle), or multiple wavelets (right). Different wavefronts are represented in purple. (B) Representation of the compatibility of rotor maintenance with other mechanisms. Rotors can be initiated by wavebreaks near an ectopic focus (left) and underlie endocardial or epicardial breakthroughs (middle). A drifting rotor, whose trajectory is depicted in blue, can be the driver of multiple and apparently disorganized atrial wavelets (right).

arrhythmia.<sup>22</sup> Figure 1A shows a diagram in which the main hypotheses for AF maintenance are illustrated.

Supporters of the multiple wavelet hypothesis highlight the disorganized electrical activity during fibrillation and the presence of multiple simultaneous propagation wavelets that can be observed during AF,<sup>23,24</sup> whose complexity increases in persistent AF patients.<sup>25</sup> However, there is strong evidence for the presence of hierarchical spatio-temporal organization in AF both in animal models and in humans<sup>26–32</sup> that is inconsistent with the multiple wavelet hypothesis and suggests AF maintenance by localized sources.

Discrete atrial fibrillatory sources have been hypothesized to be either ectopic foci<sup>33,34</sup> or rotors.<sup>22</sup> Rotors are a special type of reentry pattern of activation, termed also functional reentry, as its action potential circulates around an excitable but unexcited core,<sup>35–37</sup> in contrast to anatomical reentry which pivots around an unexcitable, such as fibrotic or ischaemic, region (also note that tissue excitability is a continuum property and is not classifying functional vs. anatomical reentry). Rotors can be initiated by a focal discharge, including a sinus wave, due to a wavefront break, as illustrated in Figure 1B, and thus the focal and rotor hypotheses as AF drivers are not mutually exclusive. In addition, repetitive surface breakthrough of activations may actually be the consequence of hidden intramural reentry,<sup>38,39</sup> and the presence of drifting and fast rotors anywhere can explain the presence of multiple wavelets in their periphery. Therefore, the hypothesis that rotor is an underlying AF mechanism is compatible with both the presence of focal discharges and multiple wavelets. It is also notable that cellular and ionic, mainly potassium and calcium, channel alterations associated with AF-induced atrial remodelling have shown to accelerate and stabilize rotors, which, in turn, allow more simultaneous wavelets and a more complex fibrillatory pattern in persistent AF patients.<sup>40–42</sup>

In this review, we focus on the presence and stability of rotors as drivers of AF. In Figure 2A, we illustrate diagrammatically the hierarchical

spatiotemporal organization of activity that is expected across the atria during an AF driven by a fast rotor. According to the illustration, waves emanating from a relatively regular fast rotor intermittently block at its periphery<sup>44</sup> and give rise to an irregular, fibrillatory activity. Further away from the rotor, the activity rate has been reduced and regularity could be regained.<sup>45</sup>

### 3. Rotors in models of AF

Much of our knowledge on rotors and their role in AF is based on experiments in models, such as the Langendorff-perfused isolated hearts, and optical mapping technology that allows for an increased spatial resolution and field of view and a more reliable detection of local action potentials than electrical recordings. In an isolated sheep heart model, Mandapati *et al.*<sup>43</sup> found a highly significant correlation between the rotation period of rotors and the dominant frequency (DF) at the same sites. In Figure 2B, isochronal activation map shows a clockwise rotor spanning across the left atrial (LA) free wall of the isolated sheep heart. This rotor was pivoting at 14 Hz, which was also the highest DF (HDF) across the entire atria. The same study found that these reentrant sources were more frequently located in the posterior free wall of the LA and were associated with a left-to-right reduction in activation frequencies. Further studies found that concomitant with LA to right atrial (RA) gradients of DF,<sup>28</sup> propagation of waves was predominately from the LA to the RA,<sup>30</sup> that is, from the fast to the slow atrium (Figure 2C and D). The driving role of LA rotors in this AF model was further confirmed by Mansour *et al.*,<sup>30</sup> who showed that ablation of interatrial conduction paths decreased the DF of the RA whereas it did not modify the DF of the LA, which was typically higher.

Rotors, as functional reentries, may meander or drift. Rotor meandering can be analysed by phase transformation of action potential recordings.<sup>46</sup> The phase representation (between  $-\pi$  and  $\pi$  radians) can

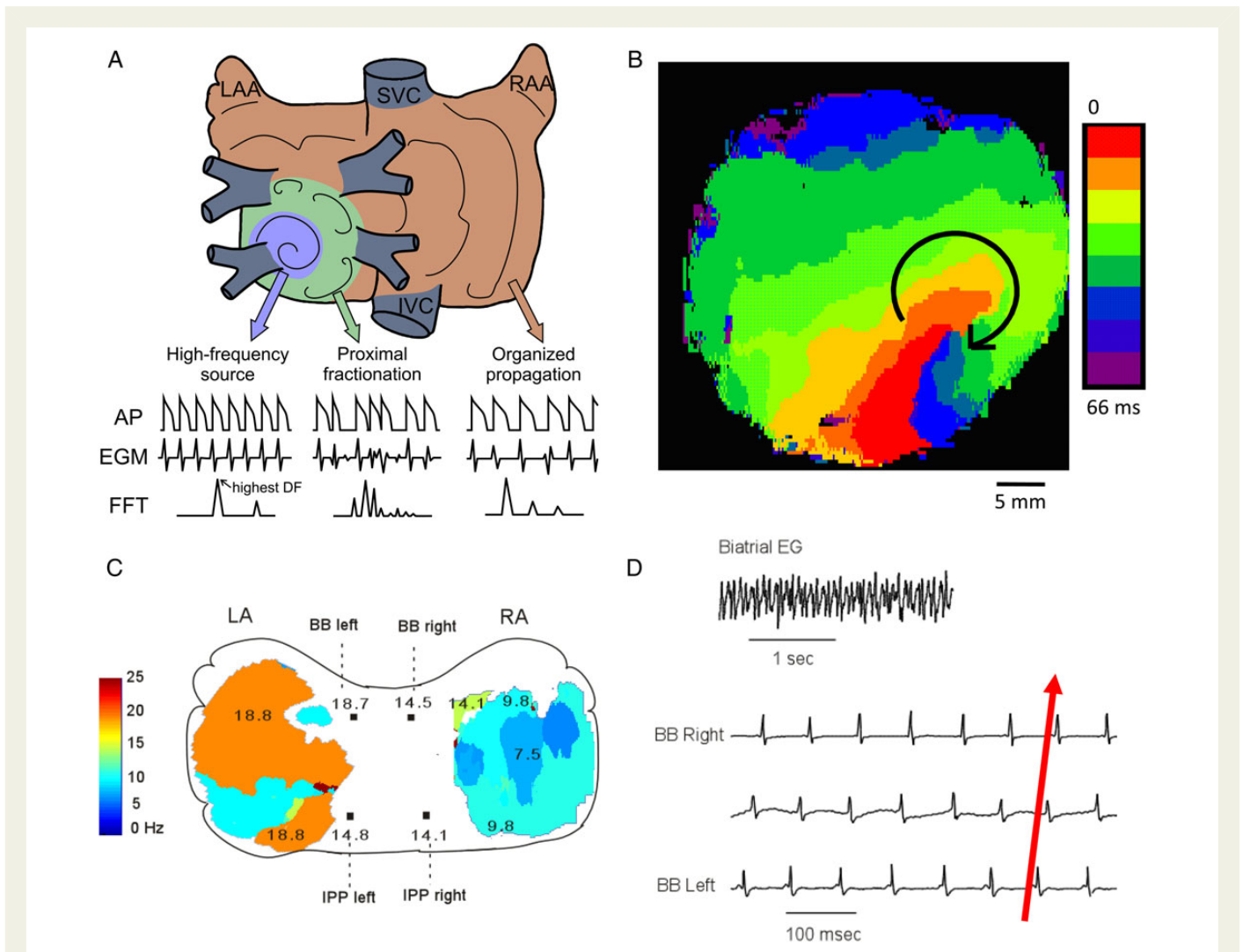


**Figure 2** Rotors and AF mechanisms. (A) Diagram of a hierarchical organization during AF driven by a fast rotor. Rotors, or reentries in general, present some spatiotemporal periodicity, and thus electrograms (EGMs) are regular. Spectral analysis identifies a dominant peak that matches the activation frequency of the rotor, which is the fastest across the atria. At the periphery of the rotor, propagation is disrupted as some activations are blocked. The variations in activation times and directions at the boundaries of the rotor result in EGMs with variable morphology and fractionation, with multiple peaks in the power spectrum. At more distal sites, the activation rate has been reduced leading to less wavebreaks and a more regular activity. (B) Isochrone map of optical activity shows an AF driver localized to the LA appendage in the form of a clockwise rotor (from Mandapati *et al.*<sup>43</sup>). (C) DF maps of epicardial surfaces of LA and RA, with values of DFs along Bachmann's bundle (BB) and infero-posterior pathway (IPP), showing a DF decrement from LA to RA. Areas of colour frequency maps indicate optical mapping field. (Small areas in red have a frequency value of 60 Hz and represent noise artefact). From Mansour *et al.*<sup>30</sup> (D) Recordings from three electrodes along BB, bottom tracing being most leftward, showing directionality of activation from LA (fast DF) to RA (slow DF) (from Mansour *et al.*<sup>30</sup>).

be computed using the Hilbert transform, which allows estimating the phase of the action potential over each cycle of the signal for varying cycle lengths, amplitudes, and morphologies. In particular, a phase map enables the identification of the wavefront without the detection of activation times and further shows its direction of propagation. Points in the phase map towards which all phases converge are designated as singularity points (SPs) and depict the instantaneous pivoting point of the wave. In Figure 3A, the sample trajectory of an SP is superimposed on an instantaneous phase map and is seen to wander over an area of  $\sim 5$  mm wide in  $\sim 2$  s. The corresponding power spectra of the SP motion illustrate that in addition to the rotor circulating at a frequency of 7.8 Hz, the meandering itself contributes a strong effect at 3.9 Hz, which was found to contribute to the irregularity of electrograms recorded

everywhere around the rotor.<sup>46</sup> In addition to meandering around a relatively fixed core, rotors may drift over larger distances. Figure 3B shows an example of such rotor drift in the LA free wall of an isolated sheep heart.<sup>47</sup> In this example, the rotor drift may have been induced by the combined effect of tissue properties and the presence of focal discharge in the vicinity of the rotor core. The rotor drift is demonstrated to cause electrogram recording fractionation as a consequence of both beat-to-beat changes in local directionality of successive activations<sup>46</sup> and the Doppler effect due to wavefront acceleration ahead of drifting rotors (illustrated in Figure 3C), giving rise to intermittent local fractionation.<sup>48</sup> In Figure 3D, we use computer simulation to illustrate this Doppler effect due to rotor drift on electrical recordings.<sup>48</sup> The drift in this simulation is based on heterogeneous distribution of the acetylcholine

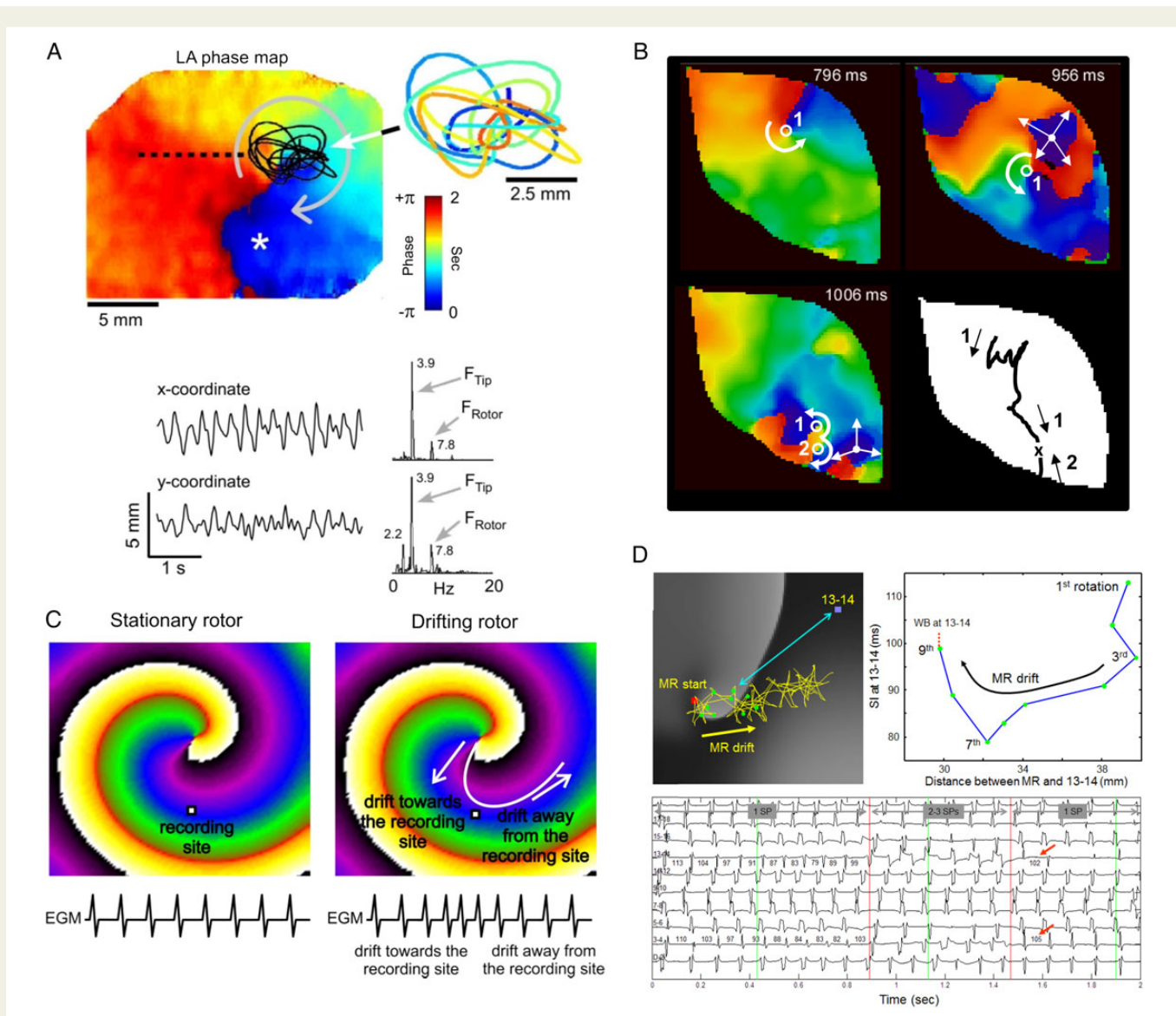


**Figure 3** Rotor meandering and drift. (A) Optical mapping phase snapshot in isolated sheep heart during AF showing reentrant activity in the LA free wall. The time–space trajectory of the tip, the x and y coordinate signals, and their corresponding spectra are shown on the right. The meandering spectral peaks ( $F_{Tip}$ ) contribute to the complexity of the local activity (from Zlochiver *et al.*<sup>46</sup>). (B) Interaction between rotors and spontaneous breakthroughs in the setting of adrenergic stimulation. A breakthrough induced substantial rotor drift as shown by corresponding PS trajectory for rotor 1, which was forced to drift downward and terminate after collision with counter-rotating rotor 2 (from Yamazaki *et al.*<sup>47</sup>). (C) Diagram illustrating that the regularity of the electrograms recorded at the vicinity of a rotor core can be related to the rotor stability. A stationary rotor gives rise to regular activation (left) as opposed to a drifting rotor (right), which results in a gradual shortening of activation times when the rotor travels towards the recording electrode and a gradual lengthening of activation times when the rotor travels away from the recording site. (D) Left: trajectory of the tip of a computer-simulated drifting rotor (MR, yellow trace) superimposed on a snapshot of voltage at time zero. Red square: starting point of the drift; green dots: the location of the tip at the completion of each of nine initial rotations; blue square: location of bipoles 13 and 14 of 20-electrode catheter recording at the top-right area of the computer model; double-headed blue arrow: distance between bipoles 13 and 14 and the tip of the rotor. Right: systolic interval (SI) at bipoles 13 and 14 as a function of distance between the tip of the rotor and the location of the bipoles. As the drifting rotor gets closer to the bipoles, SI abbreviates due to Doppler shift. After the seventh rotation, local conduction impairment at 13 and 14 increases SI with an eventual wavebreak (WB). Bottom: traces of the pseudo-bipoles from the catheter at the top-right area of the computer model. Episode of irregular electrograms appears when WB with additional SPs (three SPs) occurs (between red lines) (from Atienza *et al.*<sup>48</sup>).

(ACh)-modulated  $K^+$  inward rectifier current, whereby rotors are attracted to regions of low current density,<sup>49</sup> Therefore, from a clinical standpoint, we should be cautioned that although the rotors themselves present a certain level of organization during AF, their fast frequency, meandering, and drift result in both fibrillatory activity and irregular electrograms.

## 4. Mechanisms of rotor drift

Computer model simulations generate hypotheses on possible factors determining the rotor drifts. Numerical and theoretical studies have predicted that scroll waves, which are the three-dimensional intramural extension of the surface rotors, drift to align their axis of rotation, the

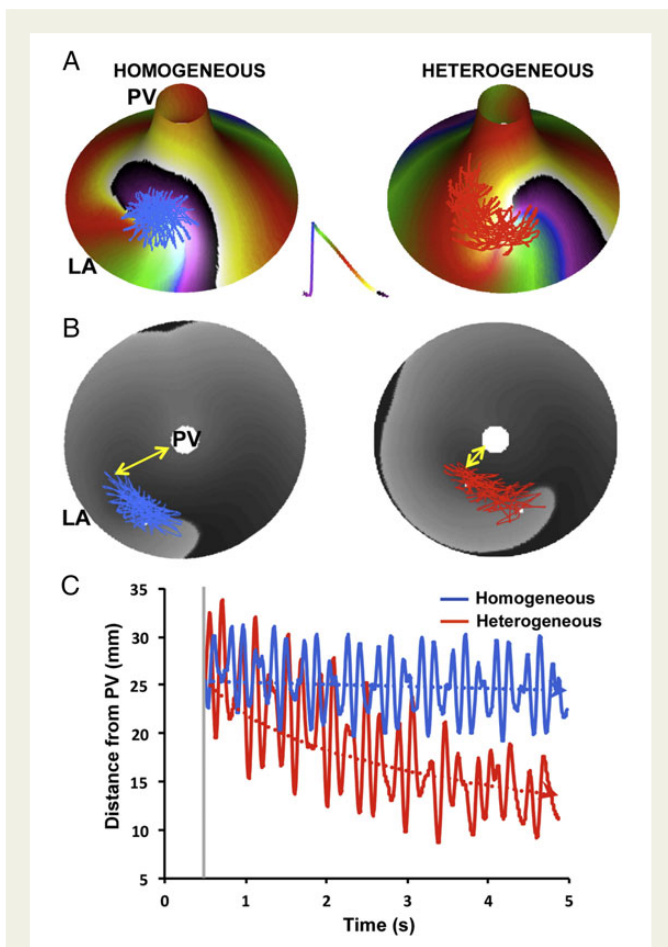


**Figure 4** Ionic mechanisms of rotor drift. (A) Funnel-shaped PV-LA models with homogeneous (left) and heterogeneous (right) ionic properties. Phase activity and SP trajectory are superimposed on the model. (B) Bull-eye view of the models in (A) with voltage snapshot (grey levels) and SP trajectories. Yellow arrows, distance between the SP and the PV. (C) The decreasing distance between the SP and the PV edge demonstrates a rotor attraction to the PV in the heterogeneous (red) but not in the homogeneous (blue) model (from Calvo et al.<sup>53</sup>).

filaments, with the minimal resistance line which approximately aligns with the myocardial fibres.<sup>50,51</sup> Other numerical studies have implicated the geometry of the atrial walls<sup>52</sup> and their ionic heterogeneities in rotor drifting and stabilization in the posterior wall of the LA. *Figure 4* shows the results of rotor drift simulations on a model of the junction between the PV and the LA [PV-LA junction (LAJ)] in a geometrical generic form of a funnel.<sup>53</sup> The simulations show that under homogeneous distribution of ionic properties, a rotor is meandering without drift, whereas under realistic heterogeneous distribution of ionic properties,<sup>54</sup> a rotor is drifting towards the PV edge of the junction model. A careful investigation of various properties of action potentials with various transmembrane currents has identified the spatial distribution of the inward potassium rectifier ( $I_{K1}$ ) as the current with the strongest effect on rotor drift in this region. The mechanisms through which  $I_{K1}$  is exerting its influence are excitability and refractoriness; rotors in the presence of sufficiently large ionic heterogeneities in those parameters have been found to always drift to where  $I_{K1}$  and excitability are minimal and refractoriness is maximal.<sup>53</sup> Although the results shown in *Figure 3*

may explain the attraction of rotors to the PV and the AF termination by PVI in some patients and are fully consistent with other studies on rotor stabilization in the atria,<sup>49,52</sup> other studies have found that rotors can be anchored to other regions as well. Both in animal models<sup>55</sup> and in human isolated hearts,<sup>56</sup> rotors seem to anchor at sites that represent boundaries of areas with different wall thicknesses<sup>55</sup> or sites with transmural differences in fibre orientation<sup>56</sup> and increased interstitial fibrosis.<sup>57</sup>

The role of some ion channel alterations associated with AF-induced remodelling in rotor dynamics has been studied in animals,<sup>40,41</sup> cell culture,<sup>42</sup> and computer<sup>58</sup> models. In a sheep model of long-term AF, an increase in DF during the transition from paroxysmal to persistent AF was associated with reduced action potential duration and densities of sodium, L-type calcium, and increased potassium inward rectifier currents, all suggesting that rotors may become more stable with the progression of AF.<sup>40,41</sup> In the same direction, Climent et al.<sup>42</sup> demonstrated that cell-culture monolayers subjected to AF-like electrical remodelling harbour an increased number of rotors with an increased spatial stability relative to baseline monolayers. In contrast, verapamil, a calcium channel blocker that reduces action potential excitability at the rotor core<sup>59</sup> and was found to lower the atrial activation frequency in persistent AF patients,<sup>60</sup> was also found to reduce rotor stability and rotation frequency, which contributed to fibrillation termination in the cell cultures.<sup>42</sup> Computer simulations suggest that the  $K^+$  inward rectifier plays a particularly important role in stabilization and acceleration of rotors in AF.<sup>58</sup> Indeed, chloroquine, a blocker of inward rectifier  $K^+$  channels, showed a similar anti-arrhythmic effect with increased rotor meandering and decreased DFs in a stretch AF model in sheep.<sup>61</sup> In fact, stretch is another variable that may affect the stability of reported AF drivers. Kalifa et al.<sup>62</sup> showed that an increase in intra-atrial pressure increases the rate and likelihood of waves emanating from the superior PVs during AF.

## 5. ACh and translation to the bedside

By performing epicardial electrical mapping in isolated canine RA, Schuessler et al.<sup>63</sup> investigated the mechanisms of tachyarrhythmias in the presence of ACh. They found that ACh-induced abbreviation of refractory period to  $<95$  ms leads to a single stable rotor that maintained the tachyarrhythmia with reduced number of simultaneous wavefronts. Sarmast et al.<sup>32</sup> subsequently demonstrated that the number of rotors, their number of rotations, and their DF in the sheep atria monotonically increased with ACh concentration, although the overall lifespan of rotors decreased. *Figure 5* shows the effect of ACh concentration on DFs in the LA and RA during AF in the isolated sheep hearts, in which both LA and RA increase their DFs with ACh concentration.<sup>32</sup>

The ACh dose-dependent acceleration of rotor frequency enabled translating animal experiments to the patients and gave the opportunity to obtain evidence, albeit indirect, for the presence of rotors as drivers in human AF through pharmacological means. Translation was made possible also by the fact that adenosine, which is widely used in the clinic, is known to activate the same Kir3.x subfamily of inward rectifier potassium channels as ACh.<sup>65–67</sup> By increasing  $K^+$  conductance in the atrium, both ACh and adenosine hyperpolarize the cell membrane, abbreviate the action potential duration and the refractory period, and thus inhibit spontaneous pacemaker discharge

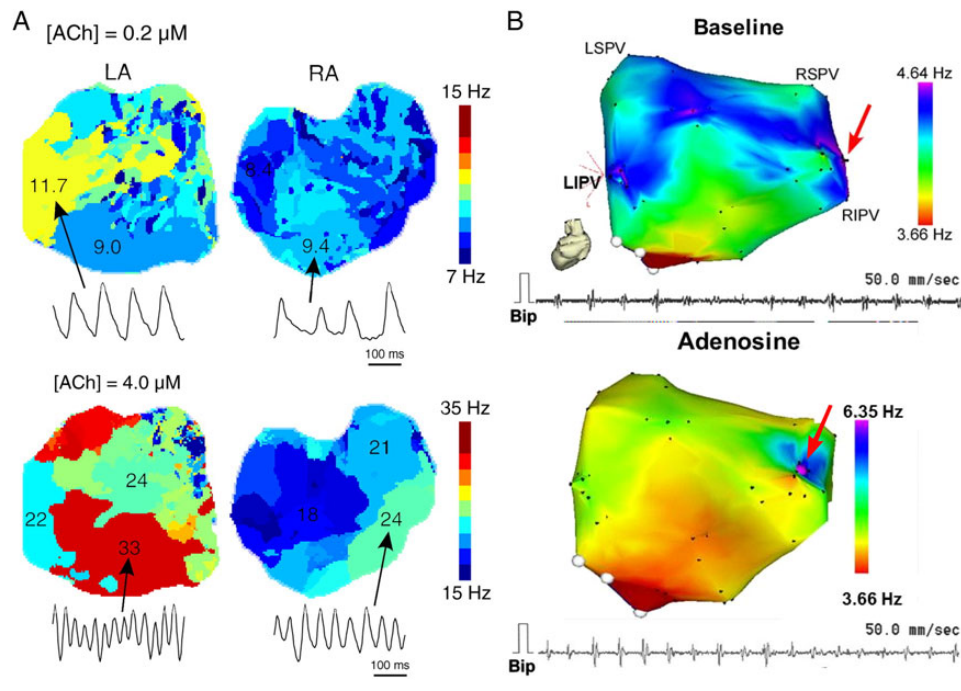


**Figure 5** Increased DF during AF with ACh and adenosine. (A) Optical mapping of the LA and RA in isolated sheep heart. (Top) At 0.2  $\mu\text{M}$  ACh, the domain frequencies as well as the frequency values and dispersion are greater in the LA than in the RA. (Bottom) At 4.0  $\mu\text{M}$  ACh, the LA to RA difference in frequency and dispersion is larger, suggesting that ACh has a more pronounced effect on the LA (from Sarmast *et al.*<sup>32</sup>). (B) LA posterior view DF map from a paroxysmal AF patient. The DF map was produced by the real-time frequency mapping CARTO system before infusion of adenosine (top), and the  $\text{DF}_{\text{max}}$  was measured again at peak adenosine effect (bottom). Red arrows indicate the primary  $\text{DF}_{\text{max}}$  site near the RIPV. DF maps and bipolar recording at the primary  $\text{DF}_{\text{max}}$  site show an increase in the DF in the presence of adenosine. LIPV, left inferior PV; RSPV, right superior PV; Bip, bipolar catheter. Reproduced from Atienza *et al.*<sup>64</sup>

as well as early and delayed depolarizations<sup>65,66</sup> but accelerate re-entrant activity.<sup>32,58</sup> We used adenosine to test the hypothesis that localized reentry maintains AF also in humans.<sup>64</sup> We determined the effects of adenosine infusion on DF at varying locations of both atria, with the idea that adenosine-induced acceleration reveals reentry as the mechanism of AF maintenance and rules out an automatic or triggered mechanism. We generated baseline DF maps of the LA using real-time spectral analysis, which allowed determination of HDF sites likely to harbour the AF drivers in AF patients.<sup>27</sup> Then the adenosine effect was measured at the primary and secondary HDF sites in the LA. *Figure 5B* shows a representative example in a paroxysmal AF patient, in which the AF frequency at baseline was  $<5$  Hz and three HDF sites were identified with the primary HDF site being located near the RIPV (red arrow). *Figure 5B* shows that the DF at the primary HDF site accelerated from 4.64 at baseline to 6.35 Hz at the peak of the adenosine effect. Interestingly, in this patient, the arrhythmia terminated during post-mapping ablation at the primary HDF site, supporting again the role of such sites as AF drivers.<sup>68</sup> Overall, adenosine infusion increased frequency primarily at sites that activated at the highest rate at baseline. In paroxysmal AF patients, adenosine increased activation frequency in the PV-LAJ. In persistent AF patients, the highest frequency sources accelerated by adenosine were located in either atria, but not at PV sites. Thus, the DF increase in response to adenosine is consistent with reentrant drivers maintaining AF that have different locations in paroxysmal compared with persistent AF patients.<sup>64</sup>

## 6. Mapping of rotors in AF patients

Initial efforts in locating rotors in human AF have used sequential or small regional mapping and rely on the mechanistic relationship between HDF sites and rotors driving AF.<sup>69</sup> Lin *et al.*<sup>70</sup> localized rotors by sequential point-by-point mapping of the atria in 53 patients. They first identified possible rotor sites in the LA as those with some degree of fractionation, HDF, and some regularity and then obtained activation maps by sequentially mapping a mean of nine sites around the putative rotor. By using this approach, they found that 15% of the paroxysmal AF patients presented activations consistent with rotors. As the mapping was sequential and conditions to qualify as rotors were stability for several minutes then, a prevalence of 15% appears to actually highlight the importance of rotors. Sanders *et al.*<sup>31</sup> demonstrated a hierarchical pattern of activation rates that was consistent with previous observations in isolated sheep hearts, with HDF sites typically located in the PV area in paroxysmal AF, although the HDF sites were more widespread in persistent AF patients. This left-to-right DF gradient in paroxysmal AF was independently verified in other laboratories as well<sup>27,64,71–74</sup> and could be attributed to a left-to-right gradient in inward rectifier potassium currents.<sup>75</sup> Atienza *et al.*<sup>27</sup> have developed a capability to determine the DF distribution in AF in real-time and showed abolishing DF gradients by ablation results in freedom of AF. Interestingly, in persistent AF, DF gradients were less prominent,<sup>27</sup> suggesting that atrial tissue remodelling possibly modifies the dynamics of AF drivers, spreading and/or multiplying them across the entire atria.<sup>31,76</sup>

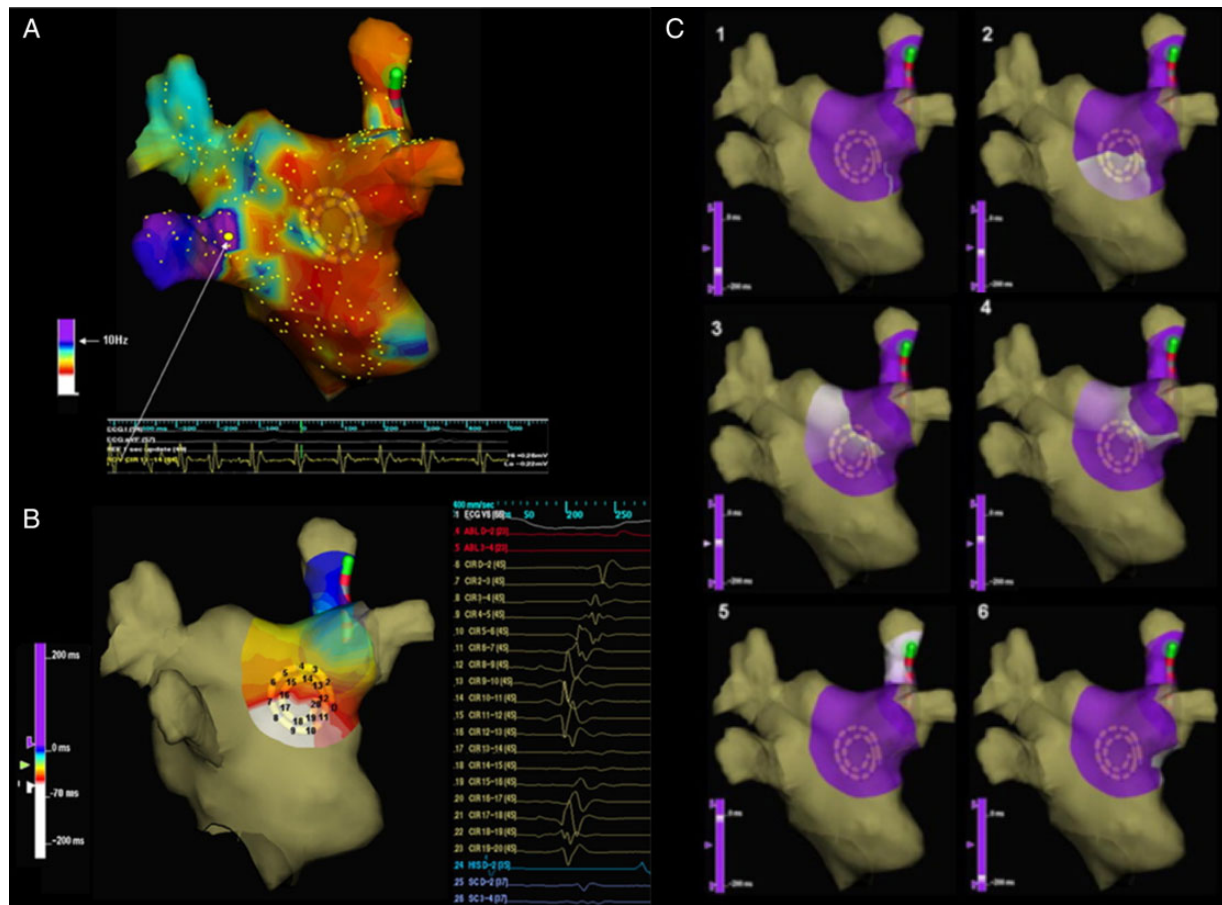


**Figure 6** Organized activation patterns in relation to DF sites. (A) LA DF map (posterior view). White arrow points to HDF site (10.8 Hz) at the left inferior PV antrum. (B) Posterior LA wall activation map during organized phase before fragmentation (right) shows an incoming wave pattern of activation progressing from closest to the HDF site at the left inferior PV (left, white) to the right (purple-blue). (C) Snapshots of wave propagation at the PLAW during transitions to fragmentation. Sequences 1–6 (purple, resting regions; white, advancing activation) show clockwise reentrant activation around a pivoting point located to the right edge of the septopulmonary bundle. From Atienza *et al.*<sup>48</sup>

First rotational activity consistent with rotors could be observed by using a multipolar spiral catheter with 20 electrodes, as shown in Figure 6.<sup>48</sup> Organized activation maps showing incoming waves that were frequently consistent with activations from the PVs accounted for 31% of the activations. Transient rotational patterns were also observed in 66% of 32 patients by Ghoraani *et al.*,<sup>77</sup> using a roving 20-pole circular catheter in the LA. However, mapping by regional multipolar catheters underestimates the number of possible rotors to be observed due to the limited atrial area simultaneously covered by the mapping catheter.

Deployment of multipolar catheters for panoramic mapping of the entire atria enabled Narayan *et al.*<sup>15,16,78</sup> to construct activation maps showing either rotational patterns or focal sources (Figure 7). This technique, termed focal impulse rotor modulation (FIRM) mapping, is based on the use of a basket-type 64-pole catheter and phase-based signal processing.<sup>79</sup> By using this approach, it was reported that as much as 97% of 101 patients presented sources in the form of focal discharges or rotors, 70% of those being rotors.<sup>16</sup> In a study with larger cohort, the same FIRM sources were identified in 258 of 260 patients (99%), for  $2.8 \pm 1.4$  sources/patient ( $1.8 \pm 1.1$  in LA and  $1.1 \pm 0.8$  in RA).<sup>80</sup> Although AF rotor cores meandered in stable regions, emanating activity presented fibrillatory conduction at the periphery of those rotors.

Each source laid in stable atrial regions for many minutes and  $4196 \pm 6360$  cycles, with no differences between paroxysmal and persistent AF ( $4290 \pm 5847$  vs.  $4150 \pm 6604$ ) or RA and LA sources.<sup>80</sup> The large prevalence of stable rotor sources reported by the FIRM approach is in contradiction with several studies, which reported no stable rotors in human AF,<sup>23,25,81,82</sup> raising skepticism on the validity of this mapping approach.<sup>79,83,84</sup> Benharash *et al.*<sup>85</sup> combined FIRM with standard electroanatomical mapping systems and reported no differences in DFs and Shannon entropy at rotor and non-rotor sites suggested by the FIRM mapping, which let the authors to conclude that FIRM observations on rotors in AF patients are not reliable.<sup>85</sup> However, the methodology in the study of Benharash *et al.* was challenged as being vastly inadequate for such discarding of the FIRM approach.<sup>86</sup>

## 7. Non-invasive mapping of rotors in human AF

The ability of body surface potentials mapping to detect rotors and stable propagation patterns during AF was described by our group.<sup>87</sup> Phase maps computed from the TQ intervals in 64 surface potentials showed

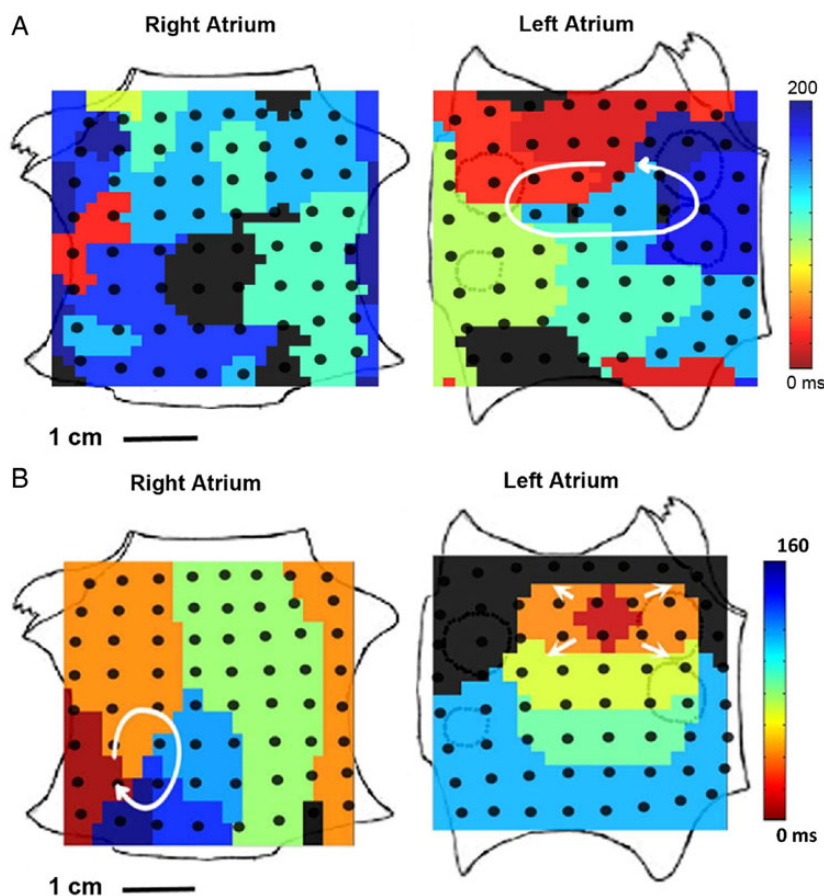


**Figure 7** Rotors driving AF in panoramic FIRM mapping in humans. (A) LA rotor with counterclockwise activation and disorganized RA during AF in a 60-year-old man. Ablation at LA rotor terminated AF to sinus rhythm in <1 min. The patient was AF free on implanted cardiac monitor at >1 year. (B) RA rotor (clockwise) and simultaneous LA focal impulse (arrowed) during persistent AF in a 47-year-old man. Ablation at RA rotor terminated AF to sinus rhythm in 5.5 min (from Narayan *et al.*<sup>16</sup>).

complex patterns in which reentries could be identified, but they were unstable and lasted for very short time. Similar observations were reported during AF using an inverse-solution electrocardiographic imaging (ECGI) system.<sup>88</sup> Patients wore a vest with 256 electrodes, and torso and heart geometries were segmented from CT images. Inverse solution was then applied to generate virtual potentials on the entire epicardial shell of the atria. Isochronal activation maps generated on the basis of virtual epicardial potentials during AF presented multiple wavelets and only 15% of patients presented activation maps that could be attributed to rotors.

Haissaguerre *et al.*<sup>89</sup> then used the ECGI system with additional signal processing that included filtering, wavelet transform, and phase mapping and observed active AF sources, which included unstable rotors and PV foci whose ablation terminated the AF. A subsequent ECGI study of 103 persistent AF patients reported up to 80.5% of activations caused by reentries with a median of 2.6 repetitive rotations (maximum 8 rotations) and a mean duration of  $449 \pm 89$  ms (Figure 8).<sup>17</sup> Although the number of rotations detected by the ECGI system is much less than that detected by the FIRM approach, the shorter-lived rotors in the ECGI mapping also tended to cluster in 1–5 discrete regions in each patient; the number of regions directly related to the duration of the AF history.<sup>17</sup>

In general, the AF activation patterns reported with the ECGI system<sup>17,89</sup> appear to be simpler than epicardial maps recorded in other studies, which do not report on the presence of rotors.<sup>25,82</sup> Although

the detection of rotors with the ECGI, and as a matter of fact any other activation pattern, during AF has not been validated to our knowledge until today using simultaneous panoramic intracardiac mapping, such a validation exists for the detection of HDF sites and interatria DF gradients using body surface potential mapping (BSPM).<sup>74</sup> Based on correlations between simultaneous real-time endocardial DF mapping and 67-electrode body surface recordings, as shown in Figure 9A, it was concluded that determining the presence of an interatria DF gradient and to identify which atrium is faster based on the surface DF distribution are possible.<sup>74</sup> As highest atrial activation frequencies can be detected from the body surface, we use this information to process and interpret our non-invasive data to study specifically driving rotors presence, which should take place at the HDFs in the atria. Figure 9B shows body surface phase maps of the grid of electrodes without and with the narrow-band filtering (2 Hz bandwidth, centred at the HDF). Although the unfiltered data (left) show multiple unstable SPs, the same data when filtered (right) show a simpler activation pattern with more stable and long-lasting rotor activity. In Figure 9C, the effect of far-field components on the instantaneous phase of surface recordings at increasing distances from the atria is illustrated. Far-field components induce potential and phase distortions that explain the large instability of non-contact phase maps. For this reason, the HDF band-pass filtering of body surface potentials distorted by components with



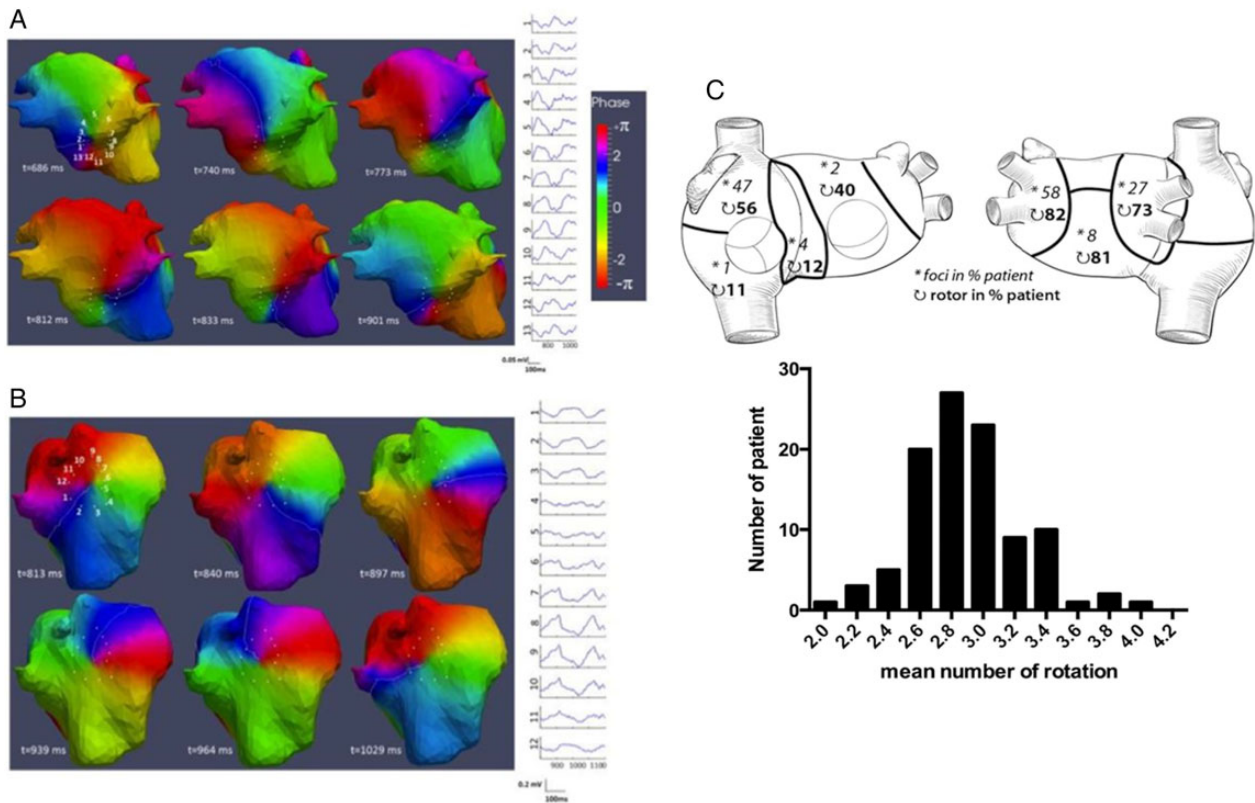


**Figure 8** Phase maps and analysis of ECGI data. (A) One of the two consecutive rotations involving the inferior LA and prephase electrograms around its core (sites 1–12). (B) One of the two consecutive rotations involving the posterior upper RA and prephase electrograms around its core (sites 1–12). (C) Top, distribution of drivers (focal breakthroughs, asterisk; reentry events, curved arrows) in seven regions is reported as the percentage of patients. For example, 82% of the 103 patients had repetitive reentries, and 58% had repetitive focal breakthroughs in left PV-appendage region. Bottom, the bar diagram shows the distribution of the mean number of rotations in 103 patients (from Haissaguerre et al.<sup>17</sup>).

different activation frequencies increased the time with observed rotors from  $8.3 \pm 5.7\%$  at baseline to  $73.1 \pm 16.8\%$  after filtering and increased the duration of continuous visible rotation from  $160 \pm 43$  to  $342 \pm 138$  ms, respectively (Figure 9D).<sup>90</sup> Of the average HDF of  $9.2 \pm 2.3$  Hz for BSPM or  $9.3 \pm 2.0$  Hz for intracardiac recordings, the latter corresponds to an average of  $2.9 \pm 0.7$  continuous rotations per SP observed in our cohort of 14 AF patients. Our BSPM phase maps obtained after filtering the surface potentials displayed patterns that resembled in their complexity those reported by the ECGI system.<sup>17,89</sup>

## 8. Simulations for non-invasive rotors mapping interpretation

To clarify the relationship between surface mapping recordings, and subsequently the inverse-solution approach of the ECGI, and the intracardiac AF activity, and particularly the effect of filtering and phase processing, we reproduced our mapping processing in computer simulations. By using a simplified spherical model of the excitable atria surrounded by a passive torso, we could track spatiotemporally potentials and phase singularities of rotors everywhere: from the inner, atrial, to the outer, surface, spheres and all torso layers in between.<sup>90</sup> Action potential rotors simulated on the atrial sphere produce rotating potentials in the torso and their phase SPs extend into the torso to form axes of pivoting potentials termed filaments. Our simulations indicate that all SPs and rotors detected on the torso surface are the ends of

filaments originating at atrial surface rotors, thus suggesting that the BSPM rotors detected in patients are not artefacts of the methodology. But our simulations also indicate a reduced sensitivity for detection of atrial rotors from the body surface. We found that the number of SPs is reduced with distance from the atria and in some cases filaments arising from the atrial SPs did reach the outer surface. In accordance with topological theories on rotor filaments,<sup>91</sup> we found that mutual cancellation between nearby counter-rotating filaments generated a natural filter, in which not only potential mapping resolution is diminished<sup>92</sup> but also filaments arising from SPs of fibrillatory conduction decreased in number with increasing distances from the atria.<sup>90</sup> This natural filtering may explain in part why our body surface phase maps<sup>90</sup> and those produced by the ECGI system<sup>17,89</sup> are simpler when compared with the expected complexity of epicardial potentials during AF.

Our simulations also help to better understand the instability of rotors on the body surface and the strong effect of the HDF bandpass filtering on their stability (Figure 9B and D). Figure 9E illustrates that without any filtering, filaments originating at a relatively stable SP span and diverge to become unstable on the torso surface (top). Following the HDF bandpass filtering, those filaments stabilize (bottom). Analysis of simulations demonstrated that wide deflection of the rotor filament inside the torso and on its surface shared a same periodicity as the propagation pattern in the non-rotor atrial regions, and thus the electrical activity of that rotor-periphery tissue would most likely be

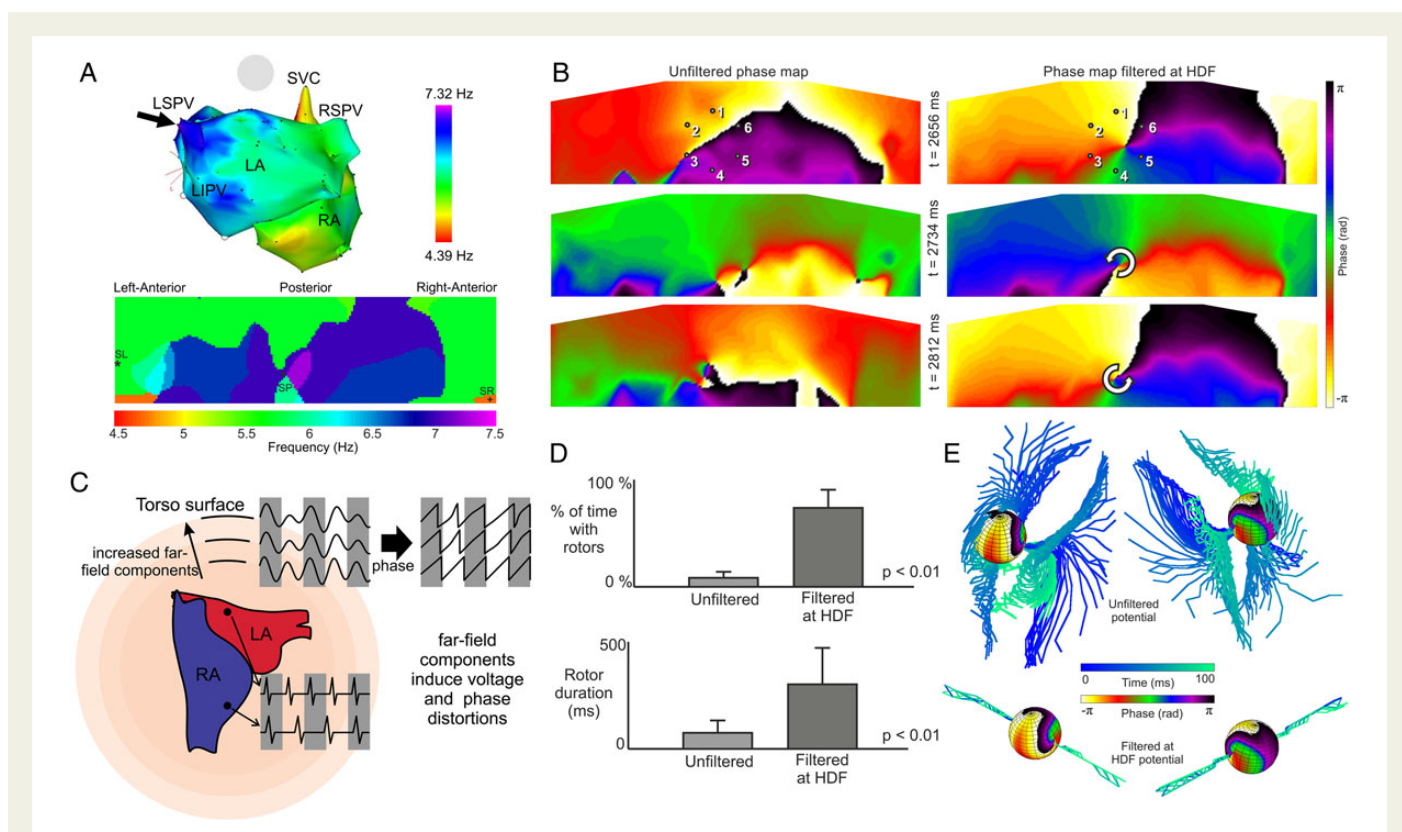


**Figure 9** Body surface DF and phase mapping. (A) Sample correlation between intracardiac and body surface DF maps. Black arrows point to the matching HDFs at the left superior PV and at the centre of the posterior body surface DF (from Guillem *et al.*<sup>74</sup>). (B) Surface phase maps at three selected times for unfiltered (left) and for HDF-filtered (right) surface potentials for a patient during AF. (C) Diagram illustrating the effect of the distance from the atrial sources and the instantaneous phase obtained from electrical recordings. The atria are depicted inside a volume conductor that represents the torso together with illustrative potentials that could be recorded at two atrial sites and at three virtual electrodes at increasing distances from the atria. At increasing distances from the atrial surface, distances from all atrial tissues become comparable and thus there are increasing far-field effects on the electrical recordings. The instantaneous phase of these electrical recordings is in turn also distorted. (D) Percentage of time with rotors (top) and rotor duration (bottom) in surface phase maps from unfiltered and HDF-filtered surface potentials over a cohort of 14 AF patients. (E) Phase map of computer-simulated epicardial sphere and temporal configuration of filaments inside the torso for unfiltered potentials and for HDF-filtered potentials (from Rodrigo *et al.*<sup>90</sup>).

the cause of filament instability.<sup>90</sup> Therefore, our HDF bandpass filtering out the effect of propagation at distal regions to the driving rotor amounts to placing the driving mechanisms of the arrhythmia under the spotlight for more accurate interpretation.

## 9. Summary and therapeutic perspectives

Rotor mapping has emerged in the recent years as a mechanistic approach for AF ablation and has opened new strategies for individual patients' basis therapies. Sanders *et al.*<sup>31</sup> were able to identify localized sites of high-frequency activity, presumably maintained by rotors, during AF in humans and showed the different DF distributions in paroxysmal and permanent AF patients, suggesting a different ablation strategy in these groups of patients. The subsequent study by Atienza *et al.*<sup>27</sup> showed that it was effective to ablate the HDF sites in order to abolish DF gradients by performing real-time DF mapping in humans. The multicentre RADAR-AF study further showed that in paroxysmal AF patients, HDF site ablation is non-inferior to the empirical isolation of PVs and was associated with a lower incidence of adverse events.<sup>14</sup>

However, in persistent AF patients, the combination of circumferential PV isolation (CPVI) with HDF site ablation offered no incremental benefit and tended to increase the complication rate.

Direct rotor-guided ablation using either endocardial or inverse computed epicardial recordings has reported higher AF freedom rates than the standard CPVI approach in persistent AF patients. Narayan *et al.*<sup>15</sup> reported a significantly improved outcome in persistent AF patients when sources identified by FIRM mapping were ablated together with a conventional anatomical ablation. Their reported success for persistent AF patients is striking: 82 vs. 45% for empirical PVI. Similar results were reported for rotor-guided ablation based on the ECGI mapping, with an 85% freedom of AF at 1 year.<sup>17</sup>

Finally, there are still open questions that will need to be addressed in the near future. Validation studies and wider use of FIRM,<sup>15</sup> ECGI,<sup>17</sup> and body surface mapping, including DF and phase methods,<sup>74,90</sup> based on ablation will help to improve AF physiology understanding and to disseminate mapping-based therapeutic approaches. For example, the relatively simple non-invasive detection of AF drivers will potentially help in selecting patients for AF ablation and planning their ablation procedures in advance. The panoramic simultaneous mapping of the atria in all the aforementioned methods is a major new feature

contributing to the understanding of AF, but it is important to note that the critical limitations in resolving the near vs. far field and the non-unique sources distribution that affects the accuracy of the methods still hinder on the ability to fully embrace those technologies for fibrillation studies. In the long run, development of new mapping technological solutions together with more realistic research models may be the key for better understanding of AF mechanisms and development of more effective therapeutic approaches.

**Conflict of interest:** M.R., A.M.C., M.S.G., F.F.-A.: none; F.A.: Advisory Board Medtronic, Sorin; O.B.: Medtronic, St Jude Medical: research grants and donations, Rhythm Solutions, Inc.: scientific officer and shareholder, and Acutus Medical, Inc.: consultant.

## Funding

This work was supported in part by grants from the Instituto de Salud Carlos III (Ministry of Economy and Competitiveness, Spain: PI13-01882, PI13-00903, and PI14/00857), Spanish Society of Cardiology (Clinical Research Grant 2015), Generalitat Valenciana (ACIF/2013/021), Innovation (Red RIC, PLE2009-0152), and NHLBI (P01-HL039707, P01-HL087226, and R01-HL118304).

## References

- Wann LS, Curtis AB, January CT, Ellenbogen KA, Lowe JE, Estes NA 3rd, Page RL, Ezekowitz MD, Slotwimer DJ, Jackman WM, Stevenson WG, Tracy CM, Writing Group M, Fuster V, Ryden LE, Cannom DS, Le Heuzey JY, Crijns HJ, Lowe JE, Curtis AB, Olsson S, Ellenbogen KA, Prystowsky EN, Halperin JL, Tamargo JL, Kay GN, Wann L, Writing Committee M, Jacobs AK, Anderson JL, Albert N, Hochman JS, Buller CE, Kushner FG, Creager MA, Ohman EM, Ettinger SM, Stevenson WG, Guyton RA, Tarkington LG, Halperin JL, Yancy CW, Members AATF. 2011 ACCF/AHA/HRS focused update on the management of patients with atrial fibrillation (updating the 2006 guideline): a report of the American College of Cardiology Foundation/American Heart Association task force on practice guidelines. *Circulation* 2011;**123**:104–123.
- Dobrev D, Nattel S. New antiarrhythmic drugs for treatment of atrial fibrillation. *Lancet* 2010;**375**:1212–1223.
- Wilber DJ, Pappone C, Neuzil P, De Paola A, Marchlinski F, Natale A, Macle L, Daoud EG, Calkins H, Hall B, Reddy V, Augello G, Reynolds MR, Vinekar C, Liu CY, Berry SM, Berry DA, ThermoCool AFII. Comparison of antiarrhythmic drug therapy and radiofrequency catheter ablation in patients with paroxysmal atrial fibrillation: a randomized controlled trial. *JAMA* 2010;**303**:333–340.
- Parkash R, Tang AS, Sapp JL, Wells G. Approach to the catheter ablation technique of paroxysmal and persistent atrial fibrillation: a meta-analysis of the randomized controlled trials. *J Cardiovasc Electrophysiol* 2011;**22**:729–738.
- Cappato R, Calkins H, Chen SA, Davies W, Ilesaka Y, Kalman J, Kim YH, Klein G, Natale A, Packer D, Skanes A, Ambrogi F, Biganzoli E. Updated worldwide survey on the methods, efficacy, and safety of catheter ablation for human atrial fibrillation. *Circ Arrhythm Electrophysiol* 2010;**3**:32–38.
- Haissaguerre M, Jais P, Shah DC, Takahashi A, Hocini M, Quiniou G, Garrigue S, Le Mouroux A, Le Metayer P, Clementy J. Spontaneous initiation of atrial fibrillation by ectopic beats originating in the pulmonary veins. *N Engl J Med* 1998;**339**:659–666.
- Calkins H, Kuck KH, Cappato R, Brugada J, Camm AJ, Chen SA, Crijns HJ, Damiano RJ Jr, Davies DW, DiMarco J, Edgerton J, Ellenbogen K, Ezekowitz MD, Haines DE, Haissaguerre M, Hindricks G, Ilesaka Y, Jackman W, Jalife J, Jais P, Kalman J, Keane D, Kim YH, Kirchhof P, Klein G, Kottkamp H, Kumagai K, Lindsay BD, Mansour M, Marchlinski FE, McCarthy PM, Mont JL, Morady F, Nademanee K, Nakagawa H, Natale A, Nattel S, Packer DL, Pappone C, Prystowsky E, Raviele A, Reddy V, Ruskin JN, Shemin RJ, Tsao HM, Wilber D. 2012 HRS/EHRA/ECAS expert consensus statement on catheter and surgical ablation of atrial fibrillation: recommendations for patient selection, procedural techniques, patient management and follow-up, definitions, endpoints, and research trial design. *Europace* 2012;**14**:528–606.
- Tzou WS, Marchlinski FE, Zado ES, Lin D, Dixit S, Callans DJ, Cooper JM, Bala R, Garcia F, Hutchinson MD, Riley MP, Verdino R, Gerstenfeld EP. Long-term outcome after successful catheter ablation of atrial fibrillation. *Circ Arrhythm Electrophysiol* 2010;**3**:237–242.
- Pappone C, Vicedomini G, Augello G, Manguso F, Saviano M, Baldi M, Petretta A, Giannelli L, Calovic Z, Guluta V, Tavazzi L, Santinelli V. Radiofrequency catheter ablation and antiarrhythmic drug therapy: a prospective, randomized, 4-year follow-up trial: the APAF study. *Circ Arrhythm Electrophysiol* 2011;**4**:808–814.
- Medi C, Sparks PB, Morton JB, Kistler PM, Halloran K, Rosso R, Vohra JK, Kumar S, Kalman JM. Pulmonary vein antral isolation for paroxysmal atrial fibrillation: results from long-term follow-up. *J Cardiovasc Electrophysiol* 2011;**22**:137–141.
- Weerasooriya R, Khairy P, Litalien J, Macle L, Hocini M, Sacher F, Lellouche N, Knecht S, Wright M, Nault I, Miyazaki S, Scavee C, Clementy J, Haissaguerre M, Jais P. Catheter ablation for atrial fibrillation: are results maintained at 5 years of follow-up? *J Am Coll Cardiol* 2011;**57**:160–166.
- Chao TF, Tsao HM, Lin YJ, Tsai CF, Lin WS, Chang SL, Lo LW, Hu YF, Tuan TC, Suenari K, Li CH, Hartono B, Chang HY, Ambrose K, Wu TJ, Chen SA. Clinical outcome of catheter ablation in patients with nonparoxysmal atrial fibrillation: results of 3-year follow-up. *Circ Arrhythm Electrophysiol* 2012;**5**:514–520.
- Dixit S, Gerstenfeld EP, Ratcliffe SJ, Cooper JM, Russo AM, Kimmel SE, Callans DJ, Lin D, Verdino RJ, Patel VV, Zado E, Marchlinski FE. Single procedure efficacy of isolating all versus arrhythmogenic pulmonary veins on long-term control of atrial fibrillation: a prospective randomized study. *Heart Rhythm* 2008;**5**:174–181.
- Atienza F, Almendral J, Ormaetxe JM, Moya A, Martinez-Alday JD, Hernandez-Madrid A, Castellanos E, Arribas F, Arias MA, Tercedor L, Peinado R, Arcocha MF, Ortiz M, Martinez-Alzamora N, Arenal A, Fernandez-Aviles F, Jalife J, RADAR-AF Investigators. Multicenter comparison of radiofrequency catheter ablation of drivers versus circumferential pulmonary vein isolation in patients with atrial fibrillation. A noninferiority randomized clinical trial. *J Am Coll Cardiol* 2014;**64**:2455–2467.
- Narayan SM, Krummen DE, Clopton P, Shivkumar K, Miller JM. Direct or coincidental elimination of stable rotors or focal sources may explain successful atrial fibrillation ablation: on-treatment analysis of the CONFIRM trial (Conventional Ablation for AF with or Without Focal Impulse and Rotor Modulation). *J Am Coll Cardiol* 2013;**62**:138–147.
- Narayan SM, Krummen DE, Shivkumar K, Clopton P, Rappel WJ, Miller JM. Treatment of atrial fibrillation by the ablation of localized sources: CONFIRM (Conventional Ablation for Atrial Fibrillation with or Without Focal Impulse and Rotor Modulation) trial. *J Am Coll Cardiol* 2012;**60**:628–636.
- Haissaguerre M, Hocini M, Denis A, Shah AJ, Komatsu Y, Yamashita S, Daly M, Amraoui S, Zellerhoff S, Picat MQ, Quotb A, Jesel L, Lim H, Ploux S, Bordachar P, Attuel G, Meillet V, Ritter P, Derval N, Sacher F, Bernus O, Cochet H, Jais P, Dubois R. Driver domains in persistent atrial fibrillation. *Circulation* 2014;**130**:530–538.
- Narayan SM, Jalife J. Crosstalk proposal: rotors have been demonstrated to drive human atrial fibrillation. *J Physiol* 2014;**592**:3163–3166.
- Allessie M, de Groot N. Crosstalk opposing view: rotors have not been demonstrated to be the drivers of atrial fibrillation. *J Physiol* 2014;**592**:3167–3170.
- Moe GK. On the multiple wavelet hypothesis of atrial fibrillation. *Arch Int Pharmacodyn* 1962;**CXL**:183–188.
- Allessie MA, Lammers WJEP, Bonke FIM, Hollen J. Experimental evaluation of Moe's wavelet hypothesis of atrial fibrillation. In: Zipes DP, Jalife J, eds. *Cardiac Electrophysiology and Arrhythmias*. Orlando: Grune & Stratton; 1985. p265–275.
- Jalife J, Berenfeld O, Mansour M. Mother rotors and fibrillatory conduction: a mechanism of atrial fibrillation. *Cardiovasc Res* 2002;**54**:204–216.
- Konings KT, Kirchhof CJ, Smeets JR, Wellens HJ, Penn OC, Allessie MA. High-density mapping of electrically induced atrial fibrillation in humans. *Circulation* 1994;**89**:1665–1680.
- Eckstein J, Zeemering S, Linz D, Maesen B, Verheule S, van Hunnik A, Crijns H, Allessie MA, Schotten U. Transmural conduction is the predominant mechanism of breakthrough during atrial fibrillation: evidence from simultaneous endo-epicardial high-density activation mapping. *Circ Arrhythm Electrophysiol* 2013;**6**:334–341.
- de Groot NM, Houben RP, Smeets JL, Boersma E, Schotten U, Schalij MJ, Crijns H, Allessie MA. Electropathological substrate of longstanding persistent atrial fibrillation in patients with structural heart disease: epicardial breakthrough. *Circulation* 2010;**122**:1674–1682.
- Gerstenfeld EP, Sahakian AV, Swiryn S. Evidence for transient linking of atrial excitation during atrial fibrillation in humans. *Circulation* 1992;**86**:375–382.
- Atienza F, Almendral J, Jalife J, Zlochiver S, Ploutz-Snyder R, Torrecilla EG, Arenal A, Kalifa J, Fernandez-Aviles F, Berenfeld O. Real-time dominant frequency mapping and ablation of dominant frequency sites in atrial fibrillation with left-to-right frequency gradients predicts long-term maintenance of sinus rhythm. *Heart Rhythm* 2009;**6**:33–40.
- Berenfeld O, Mandapati R, Dixit S, Skanes AC, Chen J, Mansour M, Jalife J. Spatially distributed dominant excitation frequencies reveal hidden organization in atrial fibrillation in the Langendorff-perfused sheep heart. *J Cardiovasc Electrophysiol* 2000;**11**:869–879.
- Chen J, Mandapati R, Berenfeld O, Skanes AC, Gray RA, Jalife J. Dynamics of wavelets and their role in atrial fibrillation in the isolated sheep heart. *Cardiovasc Res* 2000;**48**:220–232.
- Mansour M, Mandapati R, Berenfeld O, Chen J, Samie FH, Jalife J. Left-to-right gradient of atrial frequencies during acute atrial fibrillation in the isolated sheep heart. *Circulation* 2001;**103**:2631–2636.
- Sanders P, Berenfeld O, Hocini M, Jais P, Vaidyanathan R, Hsu LF, Garrigue S, Takahashi Y, Rotter M, Sacher F, Scavee C, Ploutz-Snyder R, Jalife J, Haissaguerre M. Spectral analysis identifies sites of high-frequency activity maintaining atrial fibrillation in humans. *Circulation* 2005;**112**:789–797.
- Sarmast F, Kolli A, Zaitsev A, Parisian K, Dharmoon AS, Guha PK, Warren M, Anunomwo JMB, Taffet SM, Berenfeld O, Jalife J. Cholinergic atrial fibrillation: I(K,ACH) gradients determine unequal left/right atrial frequencies and rotor dynamics. *Cardiovasc Res* 2003;**59**:863–873.

33. Jais P, Haissaguerre M, Shah DC, Chouairi S, Gencel L, Hocini M, Clementy J. A focal source of atrial fibrillation treated by discrete radiofrequency ablation. *Circulation* 1997; **95**:572–576.
34. Schmitt C, Ndrepepa G, Weber S, Schmieder S, Weyerbrock S, Schneider M, Karch MR, Deisenhofer I, Schrieck J, Zrenner B, Schomig A. Batrial multisite mapping of atrial premature complexes triggering onset of atrial fibrillation. *Am J Cardiol* 2002; **89**: 1381–1387.
35. Gray RA, Jalife J, Panfilov AV, Baxter WT, Cabo C, Davidenko JM, Pertsov AM. Mechanisms of cardiac fibrillation. *Science* 1995; **270**:1222–1223.
36. Cabo C, Pertsov AM, Davidenko JM, Baxter WT, Gray RA, Jalife J. Vortex shedding as a precursor of turbulent electrical activity in cardiac muscle. *Biophys J* 1996; **70**: 1105–1111.
37. Irvanian S, Nabutovsky Y, Kong CR, Saha S, Bursac N, Tung L. Functional reentry in cultured monolayers of neonatal rat cardiac cells. *Am J Physiol Heart Circ Physiol* 2003; **285**:H449–H456.
38. Baxter WT, Mironov SF, Zaitsev AV, Jalife J, Pertsov AM. Visualizing excitation waves inside cardiac muscle using transillumination. *Biophys J* 2001; **80**:516–530.
39. Yamazaki M, Filgueiras-Rama D, Berenfeld O, Kalifa J. Ectopic and reentrant activation patterns in the posterior left atrium during stretch-related atrial fibrillation. *Prog Biophys Mol Biol* 2012; **110**:269–277.
40. Filgueiras-Rama D, Price NF, Martins RP, Yamazaki M, Avula UM, Kaur K, Kalifa J, Ennis SR, Hwang E, Devabhaktuni V, Jalife J, Berenfeld O. Long-term frequency gradients during persistent atrial fibrillation in sheep are associated with stable sources in the left atrium. *Circ Arrhythm Electrophysiol* 2012; **5**:1160–1167.
41. Martins RP, Kaur K, Hwang E, Ramirez RJ, Willis BC, Filgueiras-Rama D, Ennis SR, Takemoto Y, Ponce-Balbuena D, Zarzoso M, O'Connell RP, Musa H, Guerrero-Serna G, Avula UM, Swartz MF, Bhushal S, Deo M, Pandit SV, Berenfeld O, Jalife J. Dominant frequency increase rate predicts transition from paroxysmal to long-term persistent atrial fibrillation. *Circulation* 2014; **129**:1472–1482.
42. Climent AM, Guillem MS, Fuentes L, Lee P, Bollensdorff C, Fernandez-Santos ME, Suarez-Sancho S, Sanz-Ruiz R, Sanchez PL, Atienza F, Fernandez-Aviles F. The role of atrial tissue remodeling on rotor dynamics: an *in-vitro* study. *Am J Physiol Heart Circ Physiol* 2015; **309**:H1964–H1973.
43. Mandapati R, Skanes A, Chen J, Berenfeld O, Jalife J. Stable microreentrant sources as a mechanism of atrial fibrillation in the isolated sheep heart. *Circulation* 2000; **101**: 194–199.
44. Berenfeld O, Zaitsev AV, Mironov SF, Pertsov AM, Jalife J. Frequency-dependent breakdown of wave propagation into fibrillatory conduction across the pectinate muscle network in the isolated sheep right atrium. *Circ Res* 2002; **90**:1173–1180.
45. Kalifa J, Tanaka K, Zaitsev AV, Warren M, Vaidyanathan R, Auerbach D, Pandit S, Vikstrom KL, Ploutz-Snyder R, Talkachou A, Atienza F, Guiraudon G, Jalife J, Berenfeld O. Mechanisms of wave fractionation at boundaries of high-frequency excitation in the posterior left atrium of the isolated sheep heart during atrial fibrillation. *Circulation* 2006; **113**:626–633.
46. Zlochiver S, Yamazaki M, Kalifa J, Berenfeld O. Rotor meandering contributes to irregularity in electrograms during atrial fibrillation. *Heart Rhythm* 2008; **5**:846–854.
47. Yamazaki M, Vaquero LM, Hou L, Campbell K, Zlochiver S, Klos M, Mironov S, Berenfeld O, Honjo H, Kodama I, Jalife J, Kalifa J. Mechanisms of stretch-induced atrial fibrillation in the presence and the absence of adrenergic stimulation: interplay between rotors and focal discharges. *Heart Rhythm* 2009; **6**:1009–1017.
48. Atienza F, Calvo D, Almendral J, Zlochiver S, Grzeda KR, Martinez-Alzamora N, Gonzalez-Torrecilla E, Arenal A, Fernandez-Aviles F, Berenfeld O. Mechanisms of fractionated electrograms formation in the posterior left atrium during paroxysmal atrial fibrillation in humans. *J Am Coll Cardiol* 2011; **57**:1081–1092.
49. Kneller J, Zou R, Vigmond EJ, Wang Z, Leon LJ, Nattel S. Cholinergic atrial fibrillation in a computer model of a two-dimensional sheet of canine atrial cells with realistic ionic properties. *Circ Res* 2002; **90**:E73–E87.
50. Berenfeld O, Pertsov AM. Dynamics of intramural scroll waves in three-dimensional continuous myocardium with rotational anisotropy. *J Theor Biol* 1999; **199**:383–394.
51. Wellner M, Berenfeld O, Jalife J, Pertsov AM. Minimal principle for rotor filaments. *Proc Natl Acad Sci USA* 2002; **99**:8015–8018.
52. Cherry EM, Ehrlich JR, Nattel S, Fenton FH. Pulmonary vein reentry—properties and size matter: insights from a computational analysis. *Heart Rhythm* 2007; **4**:1553–1562.
53. Calvo CJ, Deo M, Zlochiver S, Millet J, Berenfeld O. Attraction of rotors to the pulmonary veins in paroxysmal atrial fibrillation: a modeling study. *Biophys J* 2014; **106**: 1811–1821.
54. Cha TJ, Ehrlich JR, Zhang L, Chartier D, Leung TK, Nattel S. Atrial tachycardia remodeling of pulmonary vein cardiomyocytes: comparison with left atrium and potential relation to arrhythmogenesis. *Circulation* 2005; **111**:728–735.
55. Yamazaki M, Mironov S, Taravant C, Brec J, Vaquero LM, Bandaru K, Avula UM, Honjo H, Kodama I, Berenfeld O, Kalifa J. Heterogeneous atrial wall thickness and stretch promote scroll waves anchoring during atrial fibrillation. *Cardiovasc Res* 2012; **94**:48–57.
56. Hansen BJ, Zhao J, Csepe TA, Moore BT, Li N, Jayne LA, Kalyanasundaram A, Lim P, Bratasz A, Powell KA, Simonetti OP, Higgins RS, Kilic A, Mohler PJ, Janssen PM, Weiss R, Hummel JD, Fedorov VV. Atrial fibrillation driven by micro-anatomic intramural re-entry revealed by simultaneous sub-epicardial and sub-endocardial optical mapping in explanted human hearts. *Eur Heart J* 2015; **36**:2390–2401.
57. Tanaka K, Zlochiver S, Vikstrom KL, Yamazaki M, Moreno J, Klos M, Zaitsev AV, Vaidyanathan R, Auerbach DS, Landas S, Guiraudon G, Jalife J, Berenfeld O, Kalifa J. Spatial distribution of fibrosis governs fibrillation wave dynamics in the posterior left atrium during heart failure. *Circ Res* 2007; **101**:839–847.
58. Pandit SV, Berenfeld O, Anumonwo J, Zaritski R, Kneller J, Nattel S, Jalife J. Ionic determinants of functional reentry in a 2-d model of human atrial cells during simulated chronic atrial fibrillation. *Biophys J* 2005; **88**:3806–3821.
59. Samie FH, Mandapati R, Gray RA, Watanabe Y, Zuur C, Beaumont J, Jalife J. A mechanism of transition from ventricular fibrillation to tachycardia: effect of calcium channel blockade on the dynamics of rotating waves. *Circ Res* 2000; **86**:684–691.
60. Bollmann A, Sonne K, Esperer HD, Toepffer I, Klein HU. Patients with persistent atrial fibrillation taking oral verapamil exhibit a lower atrial frequency on the ECG. *Ann Non-invasive Electrocardiol* 2002; **7**:92–97.
61. Filgueiras-Rama D, Martins RP, Mironov S, Yamazaki M, Calvo CJ, Ennis SR, Bandaru K, Noujaim SF, Kalifa J, Berenfeld O, Jalife J. Chloroquine terminates stretch-induced atrial fibrillation more effectively than flecainide in the sheep heart. *Circ Arrhythm Electrophysiol* 2012; **5**:561–570.
62. Kalifa J, Jalife J, Zaitsev AV, Bagwe S, Warren M, Moreno J, Berenfeld O, Nattel S. Intra-atrial pressure increases rate and organization of waves emanating from the superior pulmonary veins during atrial fibrillation. *Circulation* 2003; **108**:668–671.
63. Schuessler RB, Grayson TM, Bromberg BI, Cox JL, Boineau JP. Cholinergically mediated tachyarrhythmias induced by a single extrastimulus in the isolated canine right atrium. *Circ Res* 1992; **71**:1254–1267.
64. Atienza F, Almendral J, Moreno J, Vaidyanathan R, Talkachou A, Kalifa J, Arenal A, Villacastin JP, Torrecilla EG, Sanchez A, Ploutz-Snyder R, Jalife J, Berenfeld O. Activation of inward rectifier potassium channels accelerates atrial fibrillation in humans: evidence for a reentrant mechanism. *Circulation* 2006; **114**:2434–2442.
65. Kabell G, Buchanan LV, Gibson JK, Belardinelli L. Effects of adenosine on atrial refractoriness and arrhythmias. *Cardiovasc Res* 1994; **28**:1385–1389.
66. Belardinelli L, Shryock JC, Song Y, Wang D, Srinivas M. Ionic basis of the electrophysiological actions of adenosine on cardiomyocytes. *FASEB J* 1995; **9**:359–365.
67. Khositseth A, Clapham DE, Ackerman MJ. Intracellular signaling and regulation of cardiac ion channels. In: Zipes DP, Jalife J, eds. *Cardiac Electrophysiology—From Cell to Bedside*. Philadelphia, PA: W.B. Saunders; 2004. p33–41.
68. Sanders P, Berenfeld O, Jais P, Vaidyanathan R, Hocini M, Hsu LF, Rotter M, Takahashi Y, Jalife J, Haissaguerre M. Localization of maximal dominant frequency sources correlates with the termination of atrial fibrillation during catheter ablation. *Heart Rhythm* 2004; **1**: S12.
69. Berenfeld O. Quantifying activation frequency in atrial fibrillation to establish underlying mechanisms and ablation guidance. *Heart Rhythm* 2007; **4**:1225–1234.
70. Lin WS, Tai CT, Hsieh MH, Tsai CF, Lin YK, Tsao HM, Huang JL, Yu WC, Yang SP, Ding YA, Chang MS, Chen SA. Catheter ablation of paroxysmal atrial fibrillation initiated by non-pulmonary vein ectopy. *Circulation* 2003; **107**:3176–3183.
71. Sahadevan J, Ryu K, Peltz L, Khrestian CM, Stewart RW, Markowitz AH, Waldo AL. Epicardial mapping of chronic atrial fibrillation in patients: preliminary observations. *Circulation* 2004; **110**:3293–3299.
72. Lazar S, Dixit S, Marchlinski FE, Callans DJ, Gerstenfeld EP. Presence of left-to-right atrial frequency gradient in paroxysmal but not persistent atrial fibrillation in humans. *Circulation* 2004; **110**:3181–3186.
73. Lin YJ, Tai CT, Kao T, Tso HW, Higa S, Tsao HM, Chang SL, Hsieh MH, Chen SA. Frequency analysis in different types of paroxysmal atrial fibrillation. *J Am Coll Cardiol* 2006; **47**:1401–1407.
74. Guillem MS, Climent AM, Millet J, Arenal A, Fernandez-Aviles F, Jalife J, Atienza F, Berenfeld O. Noninvasive localization of maximal frequency sites of atrial fibrillation by body surface potential mapping. *Circ Arrhythm Electrophysiol* 2013; **6**:294–301.
75. Voigt N, Trausch A, Knaut M, Matschke K, Varro A, Van Wagoner DR, Nattel S, Ravens U, Dobrev D. Left-to-right atrial inward-rectifier potassium current gradients in patients with paroxysmal versus chronic atrial fibrillation. *Circ Arrhythm Electrophysiol* 2010; **3**:472–480.
76. Hocini M, Nault I, Wright M, Veenhuizen G, Narayan SM, Jais P, Lim KT, Knecht S, Matsuo S, Forclaz A, Miyazaki S, Jadidi A, O'Neill MD, Sacher F, Clementy J, Haissaguerre M. Disparate evolution of right and left atrial rate during ablation of long-lasting persistent atrial fibrillation. *J Am Coll Cardiol* 2010; **55**:1007–1016.
77. Ghorraani B, Dalvi R, Gizurarson S, Das M, Ha A, Suszko A, Krishnan S, Chauhan VS. Localized rotational activation in the left atrium during human atrial fibrillation: relationship to complex fractionated atrial electrograms and low-voltage zones. *Heart Rhythm* 2013; **10**:1830–1838.
78. Narayan SM, Shivkumar K, Krummen DE, Miller JM, Rappel WJ. Panoramic electrophysiological mapping but not electrogram morphology identifies stable sources for human atrial fibrillation: stable atrial fibrillation rotors and focal sources relate poorly to fractionated electrograms. *Circ Arrhythm Electrophysiol* 2013; **6**:58–67.
79. Berenfeld O. Oral H. The quest for rotors in atrial fibrillation: different nets catch different fishes. *Heart Rhythm* 2012; **9**:1440–1441.
80. Swarup V, Baykaner T, Rostamian A, Daubert JP, Hummel J, Krummen DE, Trikha R, Miller JM, Tomassoni GF, Narayan SM. Stability of rotors and focal sources for human atrial fibrillation: focal impulse and rotor mapping (FIRM) of AF sources and fibrillatory conduction. *J Cardiovasc Electrophysiol* 2014; **25**:1284–1292.

81. Lee G, Kumar S, Teh A, Madry A, Spence S, Larobina M, Goldblatt J, Brown R, Atkinson V, Moten S, Morton JB, Sanders P, Kistler PM, Kalman JM. Epicardial wave mapping in human long-lasting persistent atrial fibrillation: transient rotational circuits, complex wavefronts, and disorganized activity. *Eur Heart J* 2014;**35**:86–97.
82. Lee S, Sahadevan J, Khrestian CM, Durand DM, Waldo AL. High density mapping of atrial fibrillation during vagal nerve stimulation in the canine heart: restudying the Moe hypothesis. *J Cardiovasc Electrophysiol* 2013;**24**:328–335.
83. Allesie M, de Groot N. Rebuttal from Maurits Allesie and Natasja de Groot. *J Physiol* 2014;**592**:3173.
84. Narayan SM, Jalife J. Rebuttal from Sanjiv M. Narayan and Jose Jalife. *J Physiol* 2014;**592**:3171.
85. Benharash P, Buch E, Frank P, Share M, Tung R, Shivkumar K, Mandapati R. Quantitative analysis of localized sources identified by focal impulse and rotor modulation mapping in atrial fibrillation. *Circ Arrhythm Electrophysiol* 2015;**8**:554–561.
86. Jalife J, Filgueiras-Rama D, Berenfeld O. Letter by Jalife et al. regarding article 'Quantitative analysis of localized sources identified by focal impulse and rotor modulation mapping in atrial fibrillation'. *Circ Arrhythm Electrophysiol* 2015;**8**:1296–1298.
87. Guillem MS, Climent AM, Castells F, Husser D, Millet J, Arya A, Piorowski C, Bollmann A. Noninvasive mapping of human atrial fibrillation. *J Cardiovasc Electrophysiol* 2009;**20**:507–513.
88. Cuculich PS, Wang Y, Lindsay BD, Faddis MN, Schuessler RB, Damiano RJ Jr, Li L, Rudy Y. Noninvasive characterization of epicardial activation in humans with diverse atrial fibrillation patterns. *Circulation* 2010;**122**:1364–1372.
89. Haissaguerre M, Hocini M, Shah AJ, Derval N, Sacher F, Jais P, Dubois R. Noninvasive panoramic mapping of human atrial fibrillation mechanisms: a feasibility report. *J Cardiovasc Electrophysiol* 2013;**24**:711–717.
90. Rodrigo M, Guillem MS, Climent AM, Pedron-Torrecilla J, Liberos A, Millet J, Fernandez-Aviles F, Atienza F, Berenfeld O. Body surface localization of left and right atrial high-frequency rotors in atrial fibrillation patients: a clinical-computational study. *Heart Rhythm* 2014;**11**:1584–1591.
91. Pertsov AM, Wellner M, Vinson M, Jalife J. Topological constraint on scroll wave pinning. *Phys Rev Lett* 2000;**84**:2738–2741.
92. Rudy Y, Plonsey R. The eccentric spheres model as the basis for a study of the role of geometry and inhomogeneities in electrocardiography. *IEEE Trans Biomed Eng* 1979;**26**:392–399.